

Mid-21st century air quality at the urban scale under the influence of changed climate and emissions. Case studies for Paris and Stockholm.

K. Markakis¹, M. Valari¹, M. Engardt², G. Lacressonniere³, R. Vautard³ and C. Andersson²

[1] {Laboratoire de Meteorologie Dynamique, IPSL Laboratoire CEA/CNRS/UVSQ, Ecole Polytechnique, 91128 Palaiseau Cedex, France}

[2] {Swedish Meteorological and Hydrological Institute, SE-60176 Norrköping, Sweden}

Correspondence to: K. Markakis (konstantinos.markakis@lmd.polytechnique.fr)

[3] {Laboratoire des Sciences du Climat et de l'Environnement, IPSL Laboratoire CEA/CNRS/UVSQ, Orme des Merisiers, F-91191 Gif/Yvette Cedex, France}

Correspondence to: K. Markakis (konstantinos.markakis@lmd.polytechnique.fr)

Abstract

Ozone, PM₁₀ and PM_{2.5} concentrations over Paris, France and Stockholm, Sweden were modeled at 4km and 1km horizontal resolutions respectively for the present and 2050 periods employing decade-long simulations. We account for large-scale global climate change (RCP-4.5) and fine resolution bottom-up emission projections developed by local experts and quantify their impact on future pollutant concentrations. Moreover, we identify biases related to the implementation of regional scale emission projections by comparing modeled pollutant concentrations between the fine and coarse scale simulations over the study areas. We show that over urban areas with major regional contribution (e.g., the city of Stockholm) the bias related to coarse scale projections may be significant and lead to policy misclassification. Our results stress the need to better understand the mechanism of bias propagation across the modeling scales in order to design more successful local-scale strategies. We find that the impact of climate change is spatially homogeneous in both regions, implying strong regional influence. The climate benefit for ozone (daily mean and maximum) is up to -5% for Paris and -2% for Stockholm city. The climate benefit on PM_{2.5} and PM₁₀ in Paris is between -5 and -10%, while for Stockholm we estimate mixed trends of up to 3% depending on season and size class. In Stockholm, emission mitigation leads to concentration

1 reductions up to 15% for daily mean and maximum ozone and 20% for PM. Through a sensitivity
2 analysis we show that this response is entirely due to changes in emissions at the regional scale.
3 On the contrary, over the city of Paris (VOC-limited photochemical regime), local mitigation of
4 NO_x emissions increases future ozone concentrations due to ozone titration inhibition. This
5 competing trend between the respective roles of emission and climate change, results in an increase
6 in 2050 daily mean ozone by 2.5% in Paris. Climate and not emission change appears to be the
7 most influential factor for maximum ozone concentration over the city of Paris, which may be
8 particularly interesting in a health impact perspective.

10 **1 Introduction**

11 There is a growing body of literature on the projected effects of climate and emission reduction
12 scenarios on future air quality. The published research encompass an envelope of models and
13 methodologies; up to now global scale models have been extensively used to study the impact of
14 climate on tropospheric ozone at global or regional scales (Liao et al., 2006; Prather et al., 2003;
15 Szopa and Hauglustaine, 2007), while chemistry transport models (CTMs), having more advanced
16 parameterization of physical and chemical processes, are applied to study selected regions with
17 refined horizontal resolution (Andersson and Engardt, 2010; Colette et al., 2012, 2013; Katragkou
18 et al., 2011; Langner et al., 2012a; Nolte et al., 2008; Zanis et al., 2011).

19 Numerical models are used to study future evolution of air quality as they allow the evaluation of
20 the effectiveness of planned strategies to mitigate pollutants concentrations. This is particularly
21 important since it is now well established that elevated concentrations deteriorate human health
22 (Jerrett et al., 2009; Lepeule et al., 2012), while new scientific evidence indicate that pollution is
23 harmful at even lower levels than previously thought (REVIHAAP, 2013). There is an increasing
24 number of studies investigating the health effects of population exposure to specific emission
25 source types such as traffic, industry or biomass burning (REVIHAAP, 2013 and references
26 therein). Although a clear association is not established, there is evidence that living near busy
27 roads substantially increases the total burden of disease attributable to air pollution (Pascal et al.,
28 2013). In Europe, one third of the urban population resides in areas where the legislated target
29 value for PM₁₀ is exceeded (EEA, 2013).

30 The fact that today most of the world's (and Europe's) population lives in cities stresses the need
31 to resolve the variability of pollutant concentrations and provide predictions of future air quality

1 at the urban scale (Riahi et al., 2011). Up to now the principal focus of relevant research was solely
2 on the global and regional scales utilizing modeling resolutions of a few hundred (global) to a few
3 tenths (regional) of kilometers. Nevertheless, it has been repeatedly shown that coarse resolutions
4 are inadequate to resolve fine scale features (Markakis et al., 2014, 2015; Valari and Menut, 2008;
5 Vautard et al., 2007) due to insufficient representation of chemistry and the use of coarse resolution
6 emission inventories that cannot dissociate the strong emission gradients of the large urban
7 agglomerations from those at surrounding rural areas. There is still practically no information on
8 the climate-air quality interactions at the urban scale. A reason is the large computational demand
9 in refining model resolution, while maintaining large spatial coverage. Another is the fact that
10 emission scenarios at fine scale are rarely developed, since long-term projections are constrained
11 by the evolution of energy supply and demand, which is a large scale issue. Air quality projections
12 employing locally developed policy are scarce; a first attempt is described in Gidhagen et al. (2012)
13 who developed air quality projections until the near future (2030s) for the greater Stockholm
14 region in Sweden with a high resolution (4km) modeling system. The impacts were assessed in
15 terms of climate and emissions that were constructed by local experts, however the number of
16 meteorological years included was limited and emissions were projected only for the road transport
17 sector. In Markakis et al. (2014) we describe long-term air quality projections (2050) at urban scale
18 utilizing 10 year-long simulations and fine scale features such as high model resolution (4km) and
19 an emission inventory developed by local experts for the Il-de-France (IdF; an 8-department area
20 including Paris) region in France.

21 In the present assessment we implement several improvements compared to the works of Gidhagen
22 et al. (2012) for the Stockholm region and Markakis et al. (2014) for IdF, aiming to improve our
23 knowledge on the climate and pollutants emissions driven air quality responses at a refined scale.
24 Here we develop a consistent framework including identical climate and emission scenarios at
25 global and regional scales, horizon of projection (2050), number of simulation years (decade) and
26 pollutants considered (ozone, PM₁₀ and PM_{2.5}). We implement a high resolution modeling grid of
27 1km for Stockholm and 4km for the IdF region. Here (in contrast to Markakis et al. (2014)) we
28 take into account changes from large-scale global climate and fine-scale local emissions and
29 disentangle their influence in shaping local concentrations at the 2050 horizon. For Stockholm we
30 additionally quantify the contribution of the locally enforced emission reduction plan from that
31 introduced by the pan-European change in emissions. To describe the future evolution of pollutant

emissions at the city scales we rely on high-resolution bottom-up projections at the 2030 horizon developed by local experts (instead of 2020 used in Markakis et al. (2014)).

Additionally, we employ the coarse applications that have provided the boundary conditions to the fine scale simulations from which we extract the signal for ozone, PM₁₀ and PM_{2.5} of future concentration change related to the emission mitigation over the IdF and Stockholm domains. Previous research conducted in IdF (Markakis et al., 2014) indicated a possible overestimation of the ozone concentration response from coarse resolution applications in areas characterized by VOC-limited conditions. More specifically we (Markakis et al., 2014) have identified opposing signals in the projected maximum ozone concentrations, with the regional-scale application to yield large decreases while the urban-scale large increases attributed to the fact that the former implemented top-down coarse resolution emissions and portrayed Paris under NO_x-limited chemistry at present-time conditions, therefore making the city more receptive to forthcoming NO_x emission reductions, compared to the high-resolution simulation portraying a VOC-limited chemistry for Paris. Provided that coarse inventories lack the integration of local policies, this work advances on the work of Markakis et al. (2014) and Gidhagen et al. (2012) by providing the means to identify the differences risen when finer areas are investigated with the refined information of locally developed emission projections and higher resolution. This can help to answer whether there is an added value in integrating local emission-related policy to larger-scale inventories. Specifically for ozone, in order to facilitate the comparison between the scales, we examine the long-term evolution of chemical regimes by employing chemical regime indicators which are a measure of radical production/loss processes (Beekman and Vautard, 2010; Sillman et al., 2003).

2 Materials and methods

The IdF region is located in north-central France (1.25–3.58° east and 47.89–49.45° north) with a population of 11.7 million, more than two million of which live in the city of Paris. The area is situated away from the coast and is characterized by uniform and low topography, not exceeding 200m above sea level. Stockholm is located in south-eastern Sweden, with a population of 1.4 million. Stockholm is located partly on islands where the western coast of the Baltic Sea meets Lake Mälaren. Fig. 1 illustrates the modeling domains of the urban scale simulations over IdF and Stockholm regions and the boundaries of the cities of Paris and Stockholm. 10-year long

1 simulations were carried out over each domain to represent present-time (1991-2000) and mid-21st
2 century (2046-2055) air quality.

3 We note that a cross-city comparison of results is beyond the scope of this study. The two cities
4 are used as illustrative examples of large urban agglomerations that have different origins of
5 influence; Stockholm experiences the dominant contribution of non-local sources while Paris is
6 much largely affected by local emissions. We find that in Stockholm, 99% and 74% of the local
7 ozone and annual PM_{2.5} concentrations respectively, originate from non-local sources. In previous
8 work (Markakis et al., 2014) we show that in Paris ozone chemistry is strongly VOC-limited and
9 ozone concentrations are shaped by local titration. In Markakis et al. (2015) we also show that
10 PM_{2.5} related air quality in Paris is very sensitive to local emission changes.

11 12 **2.1 Regional downscaling of climate and air quality data**

13 The air-quality simulations for the IdF and Stockholm regions were conducted to support urban
14 scale health impact assessment under the framework of the ACCEPTED (“Assessment of changing
15 conditions, environmental policies, time-activities, exposure and disease”) project. Table 1
16 summarizes the chain of models and configurations utilized for the two case studies. To derive
17 projections of the main climate drivers over Europe at 0.11° horizontal resolution (see Giorgi et al.
18 (2009)), we used the IPSL-CM5A-MR (Dufresne et al., 2013) global climate model downscaled
19 with the WRF regional climate model (Skamarock and Klemp, 2008) for the IdF region and the
20 EC-EARTH global climate model, downscaled with the RCA4 regional climate model (Jacob et
21 al., 2014; Strandberg et al., 2014) for Stockholm. In total, 8 (for present and future) meteorological
22 simulations were implemented in this study.

23 For both case studies, pollutant concentrations at the global scale were simulated (Szopa et al.,
24 2013) with the LMDz-INCA global model (Hauglustaine et al., 2004) at monthly temporal
25 resolution. The regional downscaling of multi-year pollutant concentration averages though, is
26 done separately for each case study, first over 0.44° (~50km) resolution grids over Europe and then
27 with a single nest over a 4km resolution grid over the IdF region and a two-step nesting over grids
28 of 0.11° (~12km) and 1km resolution over Sweden and Stockholm respectively (6 simulations in
29 total were conducted at present day conditions). A thorough presentation of the regional scale air
30 quality simulations used as boundary conditions for the urban scale runs are provided in Watson
31 et al. (2015).

Two sets of simulations (for each scale) were conducted at future conditions; in the first case we implement future meteorology along with present-time emissions in order to isolate the effect of climate change whereas in the second case we utilize future meteorology and projected emissions to quantify the combined effect of climate and emissions change. The signal of emission mitigation alone can be subsequently derived from the concentration difference between the two aforementioned runs (the linearity of this relationship was confirmed for the Stockholm simulations and assumed for the IdF simulations). Finally, only for the Stockholm domain we run an additional test case that allows the quantification of the contribution of emission changes at the regional scale compared to the role of the urban scale emission mitigation. This is completed using future projections of local emissions for Stockholm but keeping the respective emissions of the regional scale simulation at present-time levels.

Air quality simulations were conducted with the CHIMERE (Menut et al., 2013) and MATCH (Robertson et al., 1999) CTMs for the IdF and Stockholm regions respectively. CHIMERE is used at both urban and regional scales and it has been benchmarked in a number of model inter-comparison experiments (see Menut et al. (2013) and references therein). The MATCH model is applicable to scales from urban to hemispheric and has been extensively used to study the connection between climate change and air quality in Europe (e.g., Andersson and Engardt, 2010; Engardt et al., 2009; Langner et al., 2005, 2012b). Both models are used operationally for emergency preparedness, environmental surveillance and air quality forecasts at France (<http://www.prevoir.org>), Sweden (<http://www.smhi.se>) and EU (<http://www.macc.eu>).

The CHIMERE model includes gas-phase, solid-phase and aqueous chemistry, biogenic emission modeling with the Model of Emissions of Gases and Aerosols from Nature (MEGAN) (Guenther et al., 2006), dust emissions (Menut et al., 2005) and re-suspension (Vautard et al., 2005) modules. Gas-phase chemistry is based on the MELCHIOR mechanism (Lattuat, 1997) and includes more than 300 reactions of 80 gaseous species. CHIMERE treats sulfates, nitrates, ammonium, organic and black carbon, dust and sea-salt. The gas-particle partitioning is treated with ISORROPIA (Nenes et al., 1998). The secondary organic aerosol (SOA) chemistry of CHIMERE is described in Bessagnet et al. (2009).

The MATCH model includes options for data assimilation (e.g., Kahnert, 2008), modules describing aerosol microphysics (Andersson et al., 2015) and ozone- and particle-forming photochemistry considering ~60 species (Langner et al., 1998; Andersson et al., 2007, 2015) based on

Simpson et al. (2012). MATCH also includes SOA formed by oxidation of biogenic and anthropogenic volatile organic compounds (ASOA and BSOA). The SOA modeling is based on the volatility basis set (VBS) scheme in the EMEP MSC-W model (Bergström et al. (2012) with modifications from Bergström et al. (2014)). In the present study, primary organic aerosol emissions were considered non-volatile and VBS schemes were only used for “traditional” ASOA and BSOA; BVOC-emissions of isoprene and monoterpenes were calculated in the model, using the methodology of Simpson et al. (2012). A small emission of sesquiterpenes, equal to 5% of the daytime monoterpene emissions, was added (as in Bergström et al. (2014)).

2.2 Urban scale air quality modeling and emissions

In Markakis et al. (2015) we have conducted a sensitivity analysis on a decade simulation over IdF to test the response of modeled ozone and PM_{2.5} concentrations to the refinement of information related to model setup and inputs. On the basis of those findings, in the present study we implement a mesh-grid of 4km horizontal resolution (consisting of 39 grid cells in the west-east direction and 32 grid cells in the north-south direction), vertically resolved with 8 σ -p hybrid layers from the surface (999hPa) up to 5.5km (500hPa). The lowest layer is 25m thick. The 1km resolution domain, covering Stockholm, consists of 48x48 grid cells. The vertical resolution follows the layers of the driving regional climate model, distributed between 20 layers with a 60m thick surface layer.

Present-time emission estimates for the IdF region are available at a 1km resolution grid. Emissions are compiled with a bottom-up approach by the IdF environmental agency (AIRPARIF) combining a plethora of city-specific information (AIRPARIF, 2012). The spatial allocation of emissions is either source specific (e.g. locations of point sources) or completed with proxies such as high-resolution population maps and a detailed road network. The inventory has hourly source specific, temporal resolution. The compilation of present-time emission for the Stockholm region (covering an area of 30 municipalities and 2.2 million inhabitants) is also based on a bottom-up approach e.g., the estimates of total traffic volumes are primarily based on in-situ measurements and variations of vehicle composition and temporal variation of the traffic volumes are described for different road types. Vehicle fleet composition and vehicle exhaust emission factors are based on the Swedish application of the ARTEMIS (Assessment and Reliability of Transport Emission Models and Inventory Systems) model (Sjödin et al., 2006). There are also large non-tailpipe

emissions due to road, tyre and break wear. In Stockholm the non-tailpipe emissions dominate and emission factors are estimated based on local measurements (Omstedt et al., 2005; Ketzel et al., 2007). The emission database has hourly source specific, temporal resolution. More details on the emission data and how they were compiled can be found in Gidhagen et al. (2012).

2.3 Climate and regional scale emission projections

Climate follows the long-term 4.5 scenario of the Representative Concentration Pathways (RCP-4.5) that exhibits a 20% greenhouse gas emission reduction for Europe, constant population and mid-21st century global radiative forcing at 4W/m², increasing to 4.5W/m² by 2065 and stabilizing thereafter (Clarke et al., 2007). Shown in previous work (Markakis et al., 2014) this scenario represents an intermediate alternative between the pessimistic and optimistic RCPs (8.5 and 2.6 respectively) in terms of long-term temperature projection in IdF with 0.6°C increase in the 2050 annual mean temperature compared to -0.5°C for RCP-2.6 and +1.1°C for RCP-8.5.

The European scale simulations use anthropogenic emissions developed in the framework of the ECLIPSE (Evaluating the Climate and Air Quality Impacts of Short-Lived Pollutants) project (Klimont et al., 2013). It is consistent with the long-term climate projections of the RCPs but also spatial algorithms to improve the representation of short-term continental and national air quality legislations. In this study we used the “Current Legislation Emission” scenario (CLE) for mid-21st century in Europe, which includes both climate and regional air quality policies and assumes full enforcement of all legislated control technologies until 2030 and no climate policy thereafter. CLE projects that NO_x, NMVOCs, PM₁₀ and PM_{2.5} emissions drop in 2050 by 43, 35, 32 and 32% respectively compared to the present day. The MATCH simulations include biomass burning emissions as well taken from the Atmospheric Chemistry and Climate Model Intercomparison Project (ACCMIP) database (Lamarque et al., 2010).

2.4 Urban-scale emission projections

The IdF region with the support of the “Direction Regionale et Interdepartementale de l’Environnement et de l’Energie d’Ile de France” (DRIEE-IF), has introduced the “Plan de Protection de l’Atmosphere d’Ile de France” (PPA) enforcing short and long term emission cutbacks in order to comply with the national legislation of air pollution concentration reductions. The 2030 emission projection for the IdF region includes gradual renewal of the vehicle

1 fleet according to the latest emission standards (Euro VI), increased use of public transport,
2 replacement of domestic fuel for heating with electricity and gas, new French thermal regulations
3 in buildings, aviation traffic projections and implementation of planned legislation for the
4 industrial sector. The emission projection for the county of Stockholm is founded on vehicle fleet
5 evolution and emission factors for 2030 based on the application of the ARTEMIS model (details
6 found in Gidhagen et al. (2012)). Other emissions besides the traffic-related were not changed
7 from the present to the future in Stockholm.

8 Fig. 2 illustrates the annual, sectoral emissions of NO_x , NMVOCs, PM_{10} and $\text{PM}_{2.5}$ in the IdF
9 domain for the present-time and the 2030 scenario. Present-time NO_x emissions mainly stem from
10 the transport sector (~60% of annual emissions), largely mitigated by 2030 (emissions decline
11 from 60Gg to 20Gg). The leading emitter of NMVOCs at present-time is the “use of solvents”
12 sector accounting for 49% of all-sector annual emissions. Interestingly the emissions coming from
13 this sector are hardly mitigated in the future compared to NO_x ; the corresponding reduction reaches
14 only 11%. The transport, industrial and heating sectors have important PM_{10} emission shares at
15 present day. The heating and transport sectors are strongly mitigated (reductions reach ~60%)
16 while industrial emissions are abated by only 18% mainly due to the fact that their primary origin
17 is fugitive dust released during production processes whereas the mitigation plan introduces fuel-
18 based reductions. The main contributors of annual fine particles emissions are the transport and
19 the heating sectors, both strongly mitigated by 2030 (transport sector’s emissions drop by 96%).
20 Total present-time emissions are reduced by 55% for NO_x , 32% for NMVOCs, 37% for PM_{10} and
21 54% for $\text{PM}_{2.5}$. For Stockholm about 60 and 80% of present-time NO_x and PM_{10} emissions
22 respectively stems from the road transport sector. The decrease in the future (by 16, 18 and 10%
23 for NO_x , NMVOCs and PM_{10} respectively) in domain-wide emissions is mainly a result of planned
24 renewal of the traffic fleet and stricter emission limits. Finally, as there are no urban scale emission
25 projections available for the 2030-2050 period we assume that local emissions are unchanged
26 between 2030 and 2050. Never the less this assumption is in-line with the European scale emission
27 scenario (CLE).

29 **3 Model evaluation**

30 In this section we evaluate the present day simulations at the study domains. Surface ozone
31 concentrations modeled with CHIMERE and MATCH (averaged over the ozone period which

spans from April to August) were compared against all available measurements of the air quality networks included in the high resolution domains e.g., 17 urban, 5 suburban and 8 rural sites in IdF and one urban site (Torkel Knutsson) in Stockholm. We also evaluate maximum ozone concentrations calculated from 8-hour running means (MD8hr). Modeled PM₁₀ and PM_{2.5} ground-level concentrations in summer (JJA), winter (DJF) and on annual basis are also compared to all available measurement sites in the high resolution domains: 7 urban stations in IdF and 1 urban station (Torkel Knutsson) in the Stockholm region. Results are illustrated with scatter plots in Fig. 3. For Stockholm we additionally evaluate the organic carbon (OC) and elemental carbon (EC) as well as sea salt (as sodium) using measurements conducted during the years 2002-2003 and 2013 respectively at the remote site of Aspvreten, located 70 km south-east of Stockholm. The Aspvreten site is located outside the 1km Stockholm domain therefore we use model results from the 12km resolution simulation to represent the modelled background. We note that the measurements of particulate matter for the period in question was conducted using the Tapered-Element Oscillating Microbalance (TEOM) method that has been associated with negative sampling artefacts depending on the season, location and particle size (Allen et al., 1997).

Fig. 3a shows that over the urban stations of IdF, CHIMERE overestimates daily ozone (overall bias=10%) mostly at the urban sites outside the city center; focusing on downtown monitoring sites the model bias is only 3.7% (not shown). The simulation successfully reproduces MD8hr. Overestimation of daily ozone is observed at suburban (by 14.6%) and rural (by 13.3%) stations. Discrepancies in rural ozone may be due to overproduction of isoprene emissions due to a warm modelled bias (+0.3°, not shown) or enhanced advection from the boundaries.

The evaluation of PM_{2.5} at urban stations (Fig. 3b) shows a negligible mean bias during winter but overestimation by 15.3% in the summer. Simulations in Markakis et al. (2014), where dust emissions were not included, showed an underestimation of both summer and winter period concentrations suggesting that CHIMERE might overproduce dust particles especially in the drier summer period. From the other hand a sensitivity analysis conducted with the use of reanalysis meteorology in Markakis et al. (2015) has revealed that the small wintertime PM_{2.5} bias could be due to model error compensation such as unrealistically high modelled precipitation (not shown) and possible inhibition of vertical mixing or overestimation of wintertime anthropogenic emissions. Wintertime PM₁₀ concentrations appear underestimated (Fig. 3c) provided that the enhanced wet deposition affects the larger particles more. While the exaggeration of summertime

dust emissions is also valid for PM_{10} , PM_{10} concentrations for the same period are generally well represented. It is possible that the stronger modeled winds in the summer compared to observations (not shown) affect the larger particles more, through accelerated dry deposition (Megaritis et al., 2014). The wintertime underestimation of PM_{10} concentrations is compensated by a positive autumn bias (not shown) leading to unbiased annual average concentrations.

For the Stockholm case we have first identified the regional and local contributions to ozone, PM_{10} and $\text{PM}_{2.5}$ concentrations utilizing measurements from the rural site of Norr Malma. It is sited 80km north-east of Stockholm and only slightly affected by urban plumes, therefore we use it as an indicator of the regional influence in the area. The local contribution is defined as the difference between concentrations monitored at the Torkel Knutsson (urban) and Norr Malma (rural) sites. To evaluate the modelled regional contribution, we utilize modelled concentrations at the respective sites. We note that Norr Malma site is located in the 12km resolution domain. The Stockholm city exhibits weak titration as the daily mean ozone concentrations measured at the two sites are similar (Table 2). The performance of MATCH is therefore mainly driven by the simulations at the coarser scales which overestimate nighttime ozone (not shown) due to too efficient vertical mixing during the night; this causes the MATCH model to overestimate the regional contribution in Stockholm by 17% (not shown), which also explains the major part of the positive bias at the 1km resolution simulation by 10% (Fig. 3d). On the contrary, the regional contribution in modeled MD8hr is well represented (bias <1%) leading to unbiased MD8hr in the high-resolution modeling.

Annual mean $\text{PM}_{2.5}$ concentrations are accurately reproduced (Fig. 3e) by the MATCH model over the city but summertime levels are overestimated by 14% and wintertime by 40%. This is due to a large over-production in total sea salt in the Stockholm domain, during the whole year ($+2.1\mu\text{g}/\text{m}^3$), but mostly during winter ($+3\mu\text{g}/\text{m}^3$). Despite this, an underestimation of PM_{10} concentrations by 26% is observed over the whole year (Fig. 3f). This is due to a large summertime underprediction of PM_{10} (40%), partly explained by the model's lack of aerosols of biogenic origin, which are mainly assigned to the coarse mode of the size distribution. Spores and other primary organic material have an important contribution to the speciation of the organic aerosol in northern Europe (20% to 32% of the total carbon during summer (Yttri et al., 2011)). Another possible reason is the underestimation of OC (by $1.5\mu\text{g}/\text{m}^3$) and EC (by $0.1\mu\text{g}/\text{m}^3$), which is probably due to the bias inherited by the regional scale simulations since less than 38% and 26%

of city's PM₁₀ and PM_{2.5} concentrations respectively stem from local sources (Table 2). The regional contribution to PM₁₀ concentrations based on monitor data is about 60% but due to the aforementioned reasons 17% lower based on the MATCH simulation (annual mean) mainly stemming from the summer period (-43%).

4 Climate projections for 2050

In Table 3 we show the projected domain-wide values of key meteorological variables. A warmer climate is expected in both regions. Surface temperature in IdF increases by 0.2°C in summer and 0.4°C in winter while in the Stockholm domain this trend is stronger reaching +1.3°C in summer and +1.4°C in winter. During the summer months, when ozone formation mainly occurs, no significant change in solar radiation is observed. Ground-level wintertime specific humidity rises by ~6% in IdF and by +7 and +9.7% in summer and winter respectively over Stockholm. The effect of humidity on ozone levels is ambiguous (see Jacob and Winner (2009) for a thorough discussion); elevated levels are linked with lower levels of background ozone (Johnson et al., 1999) even though some have found a weak effect in more polluted atmospheres (Aw and Kleeman, 2003). Changes in the planetary boundary layer height (PBL) affect pollutants dispersion. In IdF we observe an increase by 3.4% in PBL during the summer and decrease by 5.6% during winter. In the Stockholm domain projected changes in the PBL are less than 2%.

The precipitation rate, a regulating factor of PM concentrations, increase by 6.5% and 3.6% during summer and winter respectively in IdF whereas, summertime precipitation in the Stockholm domain decreases by 6.3% and wintertime levels increase by only 1.7%. Nitrate concentrations are expected to increase with humidity due to shift of the ammonia-nitric acid equilibrium to the aerosol phase (Seinfeld and Pandis, 2006) but to decrease due to the higher temperatures. On the other hand, sulfates increase with the warmer climate while there is evidence that elevated humidity may also lead to decrease in particle concentration by increasing the water content of particles and accelerating dry deposition rates (Megaritis et al., 2014). A warmer climate may also affect secondary organic production since semi-volatile pollutants are more prone to the gas phase under warm temperatures. Furthermore, climate change induced changes to the oxidizing capacity may cause changes to the volatility of organic gases.

5 Air quality modeling analysis

5.1 Present-time

Maps of present-time daily mean ozone concentrations (in the ozone period) and annual mean PM_{10} and $\text{PM}_{2.5}$ concentrations are illustrated in the left columns of Fig. 4 and Fig. 5 for IdF and Stockholm domain respectively. Concentrations that are spatially averaged over the cities of Paris and Stockholm (see Fig. 1) and domain-averaged concentrations that are representative of rural areas, are discussed separately. Consequently, lower ozone concentrations are found over the city-centers due to titration while higher levels are modeled at the surrounding areas due to photochemical formation (IdF) or long-range transport (Stockholm). The urban increment of daily mean ozone, defined here as the difference between the urban and the domain-averaged concentration, is $-13\mu\text{g}/\text{m}^3$ in IdF and only $-1\mu\text{g}/\text{m}^3$ in the Stockholm domain. Ozone formation in IdF is VOC-limited and therefore, titration rate over Paris is high (Markakis et al., 2014). On the contrary, ozone levels over the city of Stockholm are mainly due to transport from the boundaries and much less affected by local NO_x emission and titration (see also discussion in the previous section). Annual $\text{PM}_{2.5}$ and PM_{10} concentrations (Fig. 4e,i) are high over areas of intense anthropogenic activity such as the Charles-de-Gaulle international airport (north-east in the IdF domain), the city-centre and the suburbs of Paris due to road transport and wintertime heating emissions while local dust contributes with PM_{10} emissions to the south. The spatial pattern of $\text{PM}_{2.5}$ and PM_{10} concentrations in the Stockholm domain mainly reflects major roads, i.e. traffic emissions (Fig. 4e,i).

5.2 Future air quality at 2050 due to climate change

Fig. 4 and Fig. 5 show the future changes (compared to present-time) in daily mean ozone concentrations (over the ozone period) and annual mean PM_{10} and $\text{PM}_{2.5}$ concentrations, due i) only to climate change; ii) only to emission reductions and iii) to the combined effect of climate and emissions for IdF and Stockholm regions respectively. The spatial distribution of the ozone concentration difference between present and future reveal that despite the overall increase of mean surface temperature there is a domain-wide climate benefit for both domains. In Paris reductions in the daily and MD8hr ozone concentrations reach $\sim 5\%$ (Table 4). To some extent this is explained by the locale climate change; decrease in surface ozone despite the warmer climate has been also observed by other researchers (Coleman et al., 2014; Fiore et al., 2005; Lauwaet et al., 2014) and linked with enhanced ozone destruction through the $\text{O}_3 + \text{OH} \rightarrow \text{HO}_2 + \text{O}_2$ reaction

1 due to increase in OH radicals triggered by higher surface water vapour ($O(^1D) + H_2O \rightarrow 2OH$).
2 For Paris this is consistent with the fact that NO_x concentrations are not much affected in the future
3 ($|\Delta c| = 1.2 \mu g/m^3$) and therefore the decrease in ozone cannot be attributed to enhanced titration. The
4 increase of the summertime period PBL height could also be responsible for the declining ozone
5 trends through less dispersed primary NO_x emissions. Most probably changes in regional climate
6 are responsible for the observed trend e.g., a weakened outflow from North America which is
7 known to affect Europe through the north and western boundaries (Auvray and Bey, 2005;
8 Lacressonniere et al., 2014). This is consistent with the fact that Paris and the IdF average
9 responses are equivalent (Table 4) also evident in the Stockholm case which is known to have
10 significant regional influence. Overall ozone concentration response in the Stockholm domain is
11 negligible ($\sim 2\%$ for daily mean and MD8hr ozone) driven by the respective response at the
12 regional level (Watson et al., 2015).

13 Changes in future concentrations of particles in IdF are up to 5% and 10% for PM_{10} and $PM_{2.5}$
14 respectively, depending on season and area of focus (Paris or IdF average, Table 4). There is a
15 weak climate benefit for annual concentrations of PM over Paris and the domain, mainly due to
16 enhanced summertime precipitation. A small increase in PM concentrations over Paris is observed
17 in wintertime as a result of a shallower boundary layer and higher temperatures that positively
18 affect sulfates. PM annual concentrations over the Stockholm domain remain practically
19 unchanged; a weak decrease of 3% is only estimated during winter, and similarly to ozone it is
20 linked to regional-scale changes.

22 **5.3 Local air quality at 2050 due to emission reductions**

23 The spatial distribution of changes in mean daily ozone concentrations due to emission mitigation
24 in the IdF region reveals two opposing trends (Fig. 4c); in Paris there is an overall increase of daily
25 ozone by $4.8 \mu g/m^3$ (Table 4) despite the enforced NO_x emission mitigation. Under the VOC-
26 limited photochemical regime characterizing the city, NO_x abatement inhibits the ozone titration
27 process resulting in higher ozone levels. The magnitude of the ozone increase due to emission
28 mitigation outbalances the predicted climate benefit and the combined effect leads to an overall
29 penalty of $+1.5 \mu g/m^3$ over Paris. In contrast, the domain-wide ozone concentrations decrease by
30 $6.5 \mu g/m^3$, since ozone over the rural areas is less affected by titration (Markakis et al., 2014). It is
31 worth noting that the absolute change in the MD8hr concentration over Paris due to climate change

1 is two times higher than due to emission mitigation (Table 4). Therefore, while local emission
2 mitigation has a stronger impact on background ozone levels, climate change affects more the
3 ozone peaks (found at around 15:00LT in Paris). This may be particularly interesting from a health
4 impact assessment standpoint where the MD8hr indicator is typically implemented (Likhvar et al.,
5 2015).

6 Emission reduction policies appear to be more efficient for ozone abatement over the Stockholm
7 region, with reductions reaching ~ 11 and $\sim 13 \mu\text{g}/\text{m}^3$ for the mean and MD8hr respectively
8 indistinctively for the city and the domain-averaged concentrations (Table 4). Based on the
9 sensitivity simulations we find that the observed ozone decrease is entirely attributed to emission
10 mitigation at the regional rather than the urban scale (Table 5). We should note however, that the
11 role of local emission reductions is probably underestimated in Stockholm due to lack of non-
12 traffic emission abatement, although traffic is the main contributor to the Stockholm NO_x
13 emissions contributing by $\sim 50\%$ to the total even after the future reductions.

14 Particle concentrations are very sensitive to their primary emission changes (Markakis et al.,
15 2015). Therefore, it is not surprising that PM concentration reductions are mainly due to emission
16 mitigation in both domains (Table 4). The domain-wide annual mean in IdF declines by 7.2 and
17 $8.1 \mu\text{g}/\text{m}^3$ and in the Stockholm domain by 1.9 and $1.6 \mu\text{g}/\text{m}^3$ for PM_{10} and $\text{PM}_{2.5}$ respectively. In
18 IdF the decrease is higher over areas and seasons with high primary PM, e.g., Paris compared to
19 the rural areas of IdF (Fig. 4g,k) as well as in wintertime compared to summertime ($-8.7 \mu\text{g}/\text{m}^3$ vs.
20 $-5.8 \mu\text{g}/\text{m}^3$ respectively for annual mean $\text{PM}_{2.5}$) due to significant abatement in the heating sector.
21 In contrast, in the Stockholm domain the seasonal and spatial distribution of changes are much less
22 prominent due to the prevailing regional influence (Table 5).

23 We have assumed unchanged local-scale emissions for the 2030-2050 period. Never the less, the
24 projected concentration change in the Stockholm region is mostly affected by regional emission
25 mitigation that according to the CLE emission scenario is weak. Therefore, further mitigation of
26 urban scale emissions would not strongly affect the future concentration change in the Stockholm
27 domain. In contrast additional emission mitigation in the IdF scale would result in further
28 improvement of domain-wide ozone and $\text{PM}_{2.5}$ -related air-quality at the mid-21st century horizon.
29 However, due to highly non-linear ozone chemistry over Paris, it is difficult to make firm
30 assumptions on the nature of ozone projected changes, under additional mitigation of ozone
31 precursor emissions in the 2030-2050 period.

5.4 Future evolution of ozone chemical regimes under local and regional scale chemistry-transport modeling in Paris

In this section we study the long-term evolution of ozone chemical regimes in the city of Paris. This analysis is not performed for Stockholm where ozone concentrations are controlled by long-range transport and less by the local chemistry which determines the regime. For each simulated day in the ozone period, in both present and future decades, we determine daily average concentrations of NO_y and the ratios of O_3/NO_y , $\text{H}_2\text{O}_2/\text{NO}_y$ and $\text{H}_2\text{O}_2/\text{NO}_z$. The threshold values proposed in order to discriminate between the two chemical regimes (i.e., NO_x or VOC-limited) are 7.6ppb for NO_y (Beekman and Vautard, 2010), 5.5 for O_3/NO_y (Sillman et al., 2003), 0.12 for $\text{H}_2\text{O}_2/\text{NO}_y$ (Sillman and He, 2002) and between 0.21 and 0.41 for $\text{H}_2\text{O}_2/\text{NO}_z$ (Beekman and Vautard, 2010). The aforementioned analysis is applied on both regional (coarse-res) and urban-scale (high-res) simulations for present and future decades. Three indicators agree on a VOC-limited characterization of present-time ozone production at the urban scale simulation in agreement to the findings of Markakis et al. (2014) while only one indicator classifies the regional scale ozone simulation as VOC-limited (Fig. 6). Despite a similar trend towards a more NO_x -limited photochemistry in 2050 at both high and coarse simulations, still three out of four indicators characterize the high-resolution simulation as VOC-limited at 2050 whereas the coarse resolution is positively NO_x -limited according to all four indicators.

5.5 Policy implications based on comparison of air quality projections from high and coarse resolution modeling

Air quality projections for 2050 indicate that ozone levels in Paris will increase by 8% and 3% for daily mean and MD8hr respectively as a response to the enforced emission mitigation plan. On the contrary, the coarse resolution simulation yields 7% and 15% decrease in these metrics (Table 6). A similar inconsistency was found in Markakis et al. (2014), where the Global Energy Assessment (GEA) emission projection (Riahi et al., 2014) was used instead of the ECLIPSE inventory. ECLIPSE stands as another state-of-the-art emission inventory, explicitly designed for air quality projections in order to cope with the drawbacks (Butler et al., 2012) of their global counterparts such as the RCPs which were intended for use in global scale climate studies. As discussed in the previous section, ozone production in the coarse resolution simulation by 2050 will shift from a

VOC- to a NO_x-limited photochemical regime and therefore more responsive to reductions of NO_x emissions compared to the urban-scale simulation where the transition to NO_x-limited conditions is smoother. PM concentrations over Paris under the high-resolution modeling are expected to decrease by 21 to 46% depending on the season and particle cut-off diameter while the coarse-resolution simulation is about 10% more optimistic with reductions ranging from 34% to 55%. Both the evolution of chemical regimes and of PM concentrations are attached to the underlying emission projections. Under the coarse-scale storyline (CLE), annual emissions of NO_x over Paris drop by almost an order of magnitude while the local inventory yields a reduction of 66%. Annual PM₁₀ and PM_{2.5} emissions in Paris drop by 76% according to CLE while only by 10 and 38% respectively according to the local projection.

Given that the coarse inventory implements assessment at the large scale, its stronger mitigation over the city of Paris compared to the AIRPARIF projection is due to omission of local policy. The downscaling of coarse inventories on regional scale CTM grids passes through spatial proxies (such as land-use) to distribute emissions and the related bias induced to the air quality simulation over finer areas increases the overall bias of the application as well. The difference in the response of the regional and urban scale simulations is due, at large extent, to the spatial allocation algorithm (inherited by the RCPs) used in the compilation of both GEA and ECLIPSE databases (Riahi et al., 2011), which forces stronger (and possibly unrealistic) mitigation over the urban areas. Additionally, regional inventories assimilate regional/national legislation. In Europe the UNECE/LRTAP convention under the revised Gothenburg protocol (http://www.unece.org/fr/env/lrtap/status/lrtap_s.html) bounds the European member states (EU28) to achieve at a 2020 horizon relative to 2005 an overall reduction by 42% in NO_x emissions and 28% in NMVOCs emissions. Such reductions enhance the shift towards NO_x-limited ozone production. This remark, suggests that coarse-resolution ozone projections may be too optimistic over VOC-limited areas, mainly found in North-Western Europe (Beekman and Vautard, 2010) as well as PM projections over heavily populated urban areas. It is plausible that new updated protocols taking into account regional particularities should be implemented in European emission mitigation schemes and more credible assessments could be achieved by incorporating local policy in large scale inventories. This point is particularly relevant for areas such as Stockholm, where the regional scale mainly drives pollutant concentrations. The transfer of bias from the larger to the finer scale may lead to misclassification of local policy.

Despite the large differences in ozone concentrations simulated at regional and urban scales over the urban area of the city of Paris, rural concentrations are very similar; the projections at both scales show a decrease in ozone at 2050 at comparable magnitudes (Table 6). Therefore, fine-scale information provides little advantage in simulating rural ozone responses in agreement with Markakis et al. (2014). On the contrary, PM rural projections are very different between simulations at different resolutions (Table 6) suggesting that regional scale biases may be transferred to the finer scale run.

A final remark relates to the relative role of climate-change and emissions in future pollutant concentration projections. In contrast to the general conclusion of most recent pan-European scale studies (Colette et al., 2013; Geels et al., 2015; Lacressonniere et al., 2014; Langner et al., 2012b) we find that maximum ozone projections over Paris, modelled at the urban scale are more sensitive (based on the absolute concentration change from present day) to climate change than to emission mitigation (Sect. 5.3). This suggests that the coarse-resolution applications could overestimate the magnitude of the contribution of the future emissions mitigation to the overall ozone concentration response.

6. Conclusions

Long-term projections of air quality at the urban scale integrating local emission policies are scarce. In the present study we investigate mid-21st century ozone and particulate matter concentrations focusing on two European cities: Paris, France and Stockholm, Sweden. Using a fine resolution modeling system (4km for the IdF region and 1km for Stockholm) we quantify the contribution of emission reduction policies and of climate-change to pollutant concentration changes at the 2050 horizon. For the Stockholm region we distinguish the role of locally enforced mitigation from that of regional-scale changes in emissions (European policy). Urban scale emission changes rely on 2030 projections compiled by authorized air quality agencies at Paris and Stockholm.

The analysis of present-time ozone concentrations reveals very different photochemical conditions in the two case-studies; ozone formation in Paris is characterized as VOC-limited, with ozone titration being the main driver of concentration levels over the city, while both PM and ozone concentrations in Stockholm depend on long-range transport of pollution (96% and 74% of the local MD8hr and annual PM_{2.5} concentrations respectively originate from non-local sources).

Overall we identify an ozone (daily mean and MD8hr) climate benefit up to -5% in IdF and -2% in Stockholm city despite the overall increase in the mean surface temperatures. For IdF this is not related to changes in local titration (as NO_x concentrations are little affected by 2050) but to changes in the regional climate. Provided the dominant regional influence in Stockholm, it is not surprising that the climate change contribution to the final PM concentrations follows the weak trend observed at continental scale simulations. In IdF, PM concentrations are expected to decrease due to the wetter climate predicted for the region although the trend is very weak.

We find that the mitigation of ozone-precursor emissions implemented in the IdF region instigates spatially irregular ozone concentration changes with a benefit over the rural areas (-9% and -12% for daily mean and MD8hr respectively) while, over the urban area we observe a penalty of +8% and +3% in daily mean and MD8hr ozone concentrations respectively due to titration inhibition. Under VOC-sensitivity ozone benefit may be attained by either pushing NMVOCs mitigation over NO_x or by enforcing enough mitigation on NO_x emissions that will allow a shift of the photochemical regime towards NO_x -limited conditions prior to 2050. In contrast the local emission projection enforces NO_x over NMVOCs reductions while according to the long-term evolution of chemical regimes, studied with the use of chemical regime indicators, NO_x mitigation is not strong enough for the aforementioned shift to take place by 2050.

In Paris, the increase in the daily mean ozone due to emission changes counterbalances the climate benefit to such extent that the combined effect is an overall penalty of +2%. In contrast changes in MD8hr concentrations due to climate ($\Delta c = -4.1 \mu\text{g}/\text{m}^3$) are larger compared to those introduced by emission abatement ($\Delta c = +2.2 \mu\text{g}/\text{m}^3$), indicating that the local maximum is more sensitive to climate change while background ozone concentration levels are more sensitive to emission changes. In the Stockholm city and the domain, emission mitigation is largely influential, with reductions several times higher than those introduced by climate both for ozone and PM. Contrary to Paris, we show that this response is entirely attributed to changes at the regional scale. Finally, the cumulative effect of climate and emissions in the city of Paris reaches +2.3% for daily mean ozone, -2.4% for MD8hr ozone, -33% for PM_{10} and -45% for $\text{PM}_{2.5}$ while for the Stockholm city, -17% for daily mean ozone, -18% for MD8hr ozone, -20% for PM_{10} and -20% for $\text{PM}_{2.5}$.

Another aim of this work was to quantify the plausible added value of the assimilation of local policy into regional scale inventories. To do so, we compared pollutant concentration changes modeled over the two cities at urban scale against regional-scale simulations over the same areas

1 forced by ECLIPSE, a state of the art emission inventory designed to cope with the drawbacks of
2 inventories such as the RCPs, by assimilating air quality policy at a continental scale. Over Paris
3 the regional scale simulation is more optimistic than its urban scale counterpart. The fine scale
4 modeling yields increase in ozone over the city of Paris (by 8% and 3% for daily mean and MD8hr
5 respectively) while the regional scale modeling yields a 7% and 15% drop respectively. Regional
6 scale simulations are more optimistic for PM concentrations as well with about 10% larger
7 reductions compared to the urban scale projections. These discrepancies are a direct effect of the
8 much stricter mitigation of primary anthropogenic emissions under the ECLIPSE scenario.

9 Overall our assessment suggests that the long-term evolution of atmospheric pollution solely based
10 on regional scale emissions may lead to misclassification of the effect. The stricter mitigation in
11 ECLIPSE projections is mainly due to the spatial allocation algorithm, which assigns
12 unrealistically high mitigation over urban areas. It is plausible that new updated protocols taking
13 into account the particularities of regions should be implemented in European emission mitigation
14 schemes and that more credible assessments could be achieved by incorporating local policy to
15 those inventories. An effect, overlooked by the coarse scale modeling, is the response of MD8hr
16 ozone, a crucial input of health impact assessment studies: for Paris this metric is more prominent
17 to climate change rather than to emission mitigation.

18 For Stockholm the comparison of regional and urban scale simulations shows small discrepancies
19 given the major role of long-range transport over the area. This stresses the need to better
20 understand the mechanism of bias propagation across the modeling scales in order to design more
21 successful local-scale strategies.

22 23 **Acknowledgements**

24 This work was carried out within the ACCEPTED project, which is supported by the ERA-
25 ENVHEALTH network (grant agreement n° 219337), with funding from ANSES, ADEME,
26 BelSPO, UBA and the Swedish EPA. Part of the work was also funded by the European Union
27 Seventh Framework Programme (FP7/2007-2013) under the project 760 IMPACT2C: Quantifying
28 projected impacts under 2°C warming, grant agreement no.282746. The ECLIPSE emissions used
29 in this study have been developed by IIASA under the European Commission FP7 project
30 ECLIPSE (Project no. 282688), while additional tasks (development of the MFR scenario) where

- 1 supported by PEGASOS (Project no. 282688) and ‘Assessment of hemispheric air pollution on
- 2 EU air policy’ (contract no.07.0307/2011/605671/SER/C3).

Table 1. Models (and their implemented resolutions) used for the simulations over the study regions.

	Climate ^a		Air quality ^b	
	IdF	Stockholm	IdF	Stockholm
Global	IPSL-CM5A-MR 1.25° x 1.25°	EC-EARTH 1.125° x 1.25°	LMDz-INCA 3.75° x 1.9°	
Regional	WRF, 0.11°	RCA4, 0.11°	CHIMERE, 0.44°	MATCH, 0.44°/0.11°
Urban	Same as regional	Same as regional	CHIMERE, 4km	MATCH, 1km

a IPSL-CM5A-MR: Institute Pierre Simon Laplace-Climate Model 5A-Mid Resolution, WRF: Weather Research and Forecasting, EC-EARTH: European Centre-Earth, RCA4: Rossby Centre regional atmospheric model

b LMDz-INCA: Laboratoire de Météorologie Dynamique Zoom- INteraction avec la Chimie et les Aérosols, MATCH: Multi-scale Atmospheric Transport and Chemistry

Table 2. Quantification of the regional and local contributions to the present-time concentration levels at the city of Stockholm.

	City concentration levels ($\mu\text{g}/\text{m}^3$) ^a	Local contribution ^b	Regional contribution ^c
Ozone daily mean	62.5	-0.8	63.3
Ozone MD8hr	78.5	-3.3	81.8
PM ₁₀ annual mean	14.7	5.7	9.0
PM ₁₀ JJA mean	13.1	3.5	9.6
PM ₁₀ DJF mean	12.7	4.4	8.3
PM _{2.5} annual mean	7.3	1.9	5.4
PM _{2.5} JJA mean	6.5	1.5	5.0
PM _{2.5} DJF mean	7.7	2.0	5.7

^a based on the only available urban background station in the domain (Torkel Knutsson).

^b calculated from the concentration difference between the Torkel Knutsson and the Norr Malma sites.

^c based on measured concentrations at the Norr Malma site.

1 Table 3. Future changes in key meteorological variables in the study regions under the RCP-4.5
 2 climate scenario. Seasonal averages include both day-time and night-time values.

IdF	Summer (JJA)		Winter (DJF)	
Variable	REF	2050	REF	2050
2m temperature (°C)	18.8	+0.2	4.2	+0.4
Specific humidity (g kg ⁻¹)	7.9	+0.3	3.4	+0.2
Precipitation (kg m ⁻²)	118	+7.1	130	+4.7
Radiation (W m ⁻²)	262	-6.5	50	-1.9
10m wind speed (m s ⁻¹)	4.0	+0.2	6.8	-0.2
Boundary layer height (m)	643	+22	727	-41
Stockholm domain	Summer (JJA)		Winter (DJF)	
Variable	REF	2050	REF	2050
2m temperature (°C)	12.9	+1.3	-1.2	+1.4
Specific humidity (g kg ⁻¹)	7.7	+0.6	3.1	+0.3
Precipitation (kg m ⁻²)	223	-14	159	+2.7
Radiation (W m ⁻²)	232	-0.4	28.2	-0.7
10m wind speed (m s ⁻¹)	3.2	-0.1	4.3	-0.1
Boundary layer height (m)	673	+6	574	-11

3

Table 4. Changes in pollutants concentrations (in $\mu\text{g}/\text{m}^3$) between present (REF) and 2050 for the IdF and Stockholm regions due to climate change, emission reduction policies and their combined effect. Results are presented separately for the urban centres (Paris and Stockholm cities) and the domain averages. Ozone is averaged over the April-August period.

	Ozone		PM₁₀			PM_{2.5}		
Paris	mean	MD8hr	JJA	DJF	annual	JJA	DJF	annual
REF	60	79	22	25	25	15	19	18
clim.	-3.3	-4.1	-1.1	+0.6	-1.1	-1.5	+0.1	-1.2
emiss.	+4.8	+2.2	-4.7	-8.1	-7.2	-5.8	-8.7	-8.1
<i>clim. + emiss.</i>	<i>+1.5</i>	<i>-1.9</i>	<i>-5.8</i>	<i>-7.5</i>	<i>-8.3</i>	<i>-7.3</i>	<i>-8.6</i>	<i>-9.3</i>
IdF Domain	mean	MD8hr	JJA	DJF	annual	JJA	DJF	annual
REF	73	92	22	21	23	14	14	15
clim.	-3.7	-4.2	+0.2	-0.2	-0.7	-1.0	0.0	-1.0
emiss.	-6.5	-11.4	-4.0	-6.6	-6.3	-4.1	-6.0	-5.9
<i>clim. + emiss.</i>	<i>-10.2</i>	<i>-15.6</i>	<i>-3.8</i>	<i>-6.8</i>	<i>-7.0</i>	<i>-5.1</i>	<i>-6.0</i>	<i>-6.9</i>
Stockholm	mean	MD8hr	JJA	DJF	annual	JJA	DJF	annual
REF	72	81	7	12	10	5.3	10	7.4
clim.	-1.3	-1.7	+0.1	-0.4	0.0	0.0	-0.3	0.0
emiss.	-11	-12.7	-1.3	-2.2	-2.0	-1.0	-1.8	-1.6
<i>clim. + emiss.</i>	<i>-12.3</i>	<i>-14.4</i>	<i>-1.2</i>	<i>-2.6</i>	<i>-2.0</i>	<i>-1.0</i>	<i>-2.1</i>	<i>-1.6</i>
Stockholm domain	mean	MD8hr	JJA	DJF	annual	JJA	DJF	annual
REF	73	81.5	6.6	11	9	5	9.5	7
clim.	-1.3	-1.1	+0.1	-0.3	+0.1	0.0	-0.3	0.0
emiss.	-11.4	-13.1	-1.3	-2.3	-1.9	-1.0	-1.9	-1.6
<i>clim. + emiss.</i>	<i>-12.7</i>	<i>-14.2</i>	<i>-1.2</i>	<i>-2.6</i>	<i>-1.8</i>	<i>-1.0</i>	<i>-2.2</i>	<i>-1.6</i>

Table 5. Contribution of the emission reduction policies implemented at the local and regional scale to the future concentration changes of ozone, PM₁₀ and PM_{2.5} in the Stockholm domain.

	Ozone		PM₁₀			PM_{2.5}		
Stockholm domain	mean	MD8hr	JJA	DJF	annual	JJA	DJF	annual
REF	73	81.5	6.6	11	9	5	9.5	7
local	+0.1	+0.1	-0.1	-0.1	-0.1	0.0	0.0	0.0
regional	-11.5	-13.2	-1.2	-2.4	-1.8	-1.0	-1.9	-1.6
local+regional	-11.4	-13.1	-1.3	-2.3	-1.9	-1.0	-1.9	-1.6

1 Table 6. Future concentration response relative to present (in %) under the high and coarse-
2 resolution applications over the city of Paris and the IdF domain.

	Ozone		PM₁₀			PM_{2.5}		
	mean	MD8hr	JJA	DJF	annual	JJA	DJF	annual
Paris high-res	+8	+3	-21	-32	-32	-38	-46	-44
Paris coarse-res	-7	-15	-34	-47	-42	-43	-55	-52
IdF high-res	-9	-12	-18	-32	-27	-29	-42	-39
IdF coarse-res	-9	-16	-29	-41	-37	-39	-52	-49

3

References

- AIRPARIF: Evaluation Prospective des émissions et des concentrations des polluants atmosphériques à l'horizon 2020 en Ile-De-France – Gain sur les émissions en 2015, available at: http://www.airparif.asso.fr/_pdf/publications/ppa-rapport-121119.pdf (last access: 30 September 2015), 2012.
- Allen, G., Sioutas, C., Koutrakis, P., Reiss, R., Lurmann, F.W. and Roberts, P.T.: Evaluation of the TEOM method for measurement of ambient particulate mass in urban areas, *J. Air Waste Manag. Assoc.*, 47 (6), 682-689, 1997.
- Andersson, C., Langner, J., and Bergström, R.: Interannual variation and trends in air pollution over Europe due to climate variability during 1958-2001 simulated with a regional CTM coupled to the ERA40 reanalysis, *Tellus* 59B, 77-98. doi: 10.1111/j.1600-0889.2006.00196.x, 2007.
- Andersson, C. and Engardt, M.: European ozone in a future climate: Importance of changes in dry deposition and isoprene emissions, *J. Geophys. Res.*, 115, D02303, doi: 10.1029/2008JD011690, 2010.
- Andersson, C., Bergström, R., Bennet, C., Robertson, L., Thomas, M., Korhonen, H., Lehtinen, K.E.J. and Kokkola, H.: MATCH-SALSA – Multi-scale Atmospheric Transport and CHEMistry model coupled to the SALSA aerosol microphysics model – Part 1: Model description and evaluation, *Geosci. Model Dev.*, 8, 2015.
- Aw, J., and Kleeman, M. J.: Evaluating the first-order effect of intra-annual temperature variability on urban air pollution, *J. Geophys. Res.*, 108 (D12), 4365, doi:10.1029/2002JD002688, 2003.
- Beekmann, M. and Vautard, R.: A modeling study of photochemical regimes over Europe: robustness and variability, *Atmos. Chem. Phys.*, 10, 10067-10084, 2010.
- Bergström, R., Denier van der Gon, H.A.C., Prévôt, A.S.H., Yttri, K.E. and Simpson, D.: Modeling of organic aerosols over Europe (2002–2007) using a volatility basis set (VBS) framework: application of different assumptions regarding the formation of secondary organic aerosol, *Atmos. Chem. Phys.*, 12, 8499–8527, 2012.
- Bergström, R., Hallquist, M., Simpson, D., Wildt, J. and Mentel, T.F.: Biotic stress: a significant contributor to organic aerosol in Europe?, *Atmos. Chem. Phys.*, 14, 13643-13660, 2014.
- Bessagnet, B., Menut, L., Curci, G., Hodzic, A., Guillaume, B., Liousse, C., Moukhtar, S., Pun, B., Seigneur, C. and Schulz, M.: Regional modeling of carbonaceous aerosols over Europe – Focus on Secondary Organic Aerosols, *J. Atmos. Chem.*, 61, 175-202, 2009.

1 Coleman, L., Martin, D., Varghese, S., Jennings, S.G. and O' Dowd, C.D.: Assessment of changing
2 meteorology and emissions on air quality using a regional climate model: Impact on ozone, *Atmos.*
3 *Environ.*, 69, 198-210, 2014.

4 Colette, A., Granier, C., Hodnebrog, O., Jakobs, H., Maurizi, A., Nyiri, A., Rao, S., Amann, M.,
5 Bessagnet, B., D'Angiola, A., Gauss, M., Heyes, C., Klimont, Z. and Meleux, F.: Future air quality
6 in Europe: a multi-model assessment of projected exposure to ozone, *Atmos. Chem. Phys.*, 12,
7 10613-10630, 2012.

8 Colette, A., Bessagnet, B., Vautard, R., Szopa, S., Rao, S., Schucht, S., Klimont, Z., Menut, L.,
9 Clain, G., Meleux, F., Curci, G. and Rouïl, L.: European atmosphere in 2050, a regional air quality
10 and climate perspective under CMIP5 scenarios, *Atmos. Chem. Phys.*, 13, 7451–7471,
11 doi:10.5194/acp-13-7451-2013, 2013.

12 Clarke, L., Edmonds, J., Jacoby, H., Pitcher, H., Reilly, J. and Richels, R.: Scenarios of
13 Greenhouse Gas Emissions and Atmospheric Concentrations. Sub-report 2.1A of Synthesis and
14 Assessment Product 2.1 by the U.S. Climate Change Science Program and the Subcommittee on
15 Global Change Research. Department of Energy, Office of Biological & Environmental Research,
16 Washington, 7 DC., USA, pp. 154, 2007.

17 Deguillaume, L., Beekmann, M. and Derognat, C.: Uncertainty evaluation of ozone production
18 and its sensitivity to emission changes over the Ile-de-France region during summer periods, *J.*
19 *Geophys. Res.*, 113, D02304, doi:10.1029/2007JD009081, 2008.

20 Dufresne, J.-L., Foujols, M.-A., Denvil, S., Caubel, A., Marti, O., Aumont, O., Balkanski, Y.,
21 Bekki, S., Bellenger, H., Benshila, R., Bony, S., Bopp, L., Braconnot, P., Brockmann, P., Cadule,
22 P., Cheruy, F., Codron, F., Cozic, A., Cugnet, D., de Noblet, N., Duvel, J.-P Ethé, C., Fairhead,
23 L., Fichefet, T., Flavoni, S., Friedlingstein, P., Grandpeix, J.-Y., Guez, L., Guilyardi, E.,
24 Hauglustaine, D., Hourdin, F., Idelkadi, A., Ghattas, J., Joussaume, S., Kageyama, M., Krinner,
25 G., Labetoulle, S., Lahellec, A., Lefebvre, M.-P., Lefevre, F., Levy, C., Li, Z. X., Lloyd, J., Lott,
26 J., Madec, G., Mancip, M., Marchand, M., Masson, S., Meurdesoif, Y., Mignot, J., Musat, I.,
27 Parouty, S., Polcher, J., Rio, C., Schulz, M., Swingedouw, D., Szopa, S., Talandier, C., Terray, P.,
28 Viovy, N. and Vuichard, N.: Climate change projections using the IPSL-CM5 Earth System
29 Model: from CMIP3 to CMIP5, *Clim. Dynam.*, 40, 2123–2165, 2013.

1 Engardt, M., Bergstrom, R. and Andersson, C.: Climate and emission changes contributing to
2 changes in near-surface ozone in Europe over the coming decades: Results from model studies,
3 *Ambio* 38, 452–458. DOI: 10.1579/0044-7447-38.8.452, 2009.

4 Environmental Protection Agency (EEA): Air quality in Europe - 2013 report, available at:
5 <http://www.eea.europa.eu/publications/air-quality-in-europe-2013> (last access: 30 September
6 2015), 2013.

7 Geels, C., Andersson, C., Hänninen, O., Lansø, A.S., Schwarze, P.E., Skjøth, C.A., and Brandt, J.:
8 Future Premature Mortality Due to O₃, Secondary Inorganic Aerosols and Primary PM in Europe
9 - Sensitivity to Changes in Climate, Anthropogenic Emissions, Population and Building Stock, *Int.*
10 *J. Environ. Res. Public Health*, 12, 2837-2869, 2015.

11 Gidhagen, L., Engardt, M., Lövenheim, B. and Johansson, C.: Modeling effects of climate change
12 on air quality and population exposure in urban planning scenarios, *Advances in Meteorology*, 12
13 pages. DOI:10.1155/2012/240894, 2012.

14 Guenther, A., Karl, T., Harley, P., Wiedinmyer, C., Palmer, P.I. and Geron, C.: Estimates of global
15 terrestrial isoprene emissions using MEGAN (Model of Emissions of Gases and Aerosols from
16 Nature), *Atmos. Chem. Phys.*, 6, 3181–3210, doi:10.5194/acp-6-3181-2006, 2006.

17 Giorgi, F., Coppola, E., Solmon, F., Mariotti, L., Sylla, M.B., Bi, X., Elguindi, N., Diro, G.T.,
18 Nair, V., Giuliani, G., Turuncoglu, U.U., Cozzini, S., Güttler, L., O'Brien, T.A., Tawfik, A.B.,
19 Shalaby, A., Zakey, A.S., Steiner, A.L., Stordal, F., Sloan, L.C. and Brankovic, C.: RegCM4:
20 model description and preliminary tests over multiple CORDEX domains, *Clim. Res.*, 52: 7-29,
21 2012.

22 Hauglustaine, D. A., Hourdin, F., Jourdain, L., Filiberti, M.-A., Walters, S., Lamarque, J.F. and
23 Holland, E.A.: Interactive chemistry in the Laboratoire de Meteorologie Dynamique general
24 circulation model: Description and background tropospheric chemistry evaluation, *J. Geophys.*
25 *Res.*, 109, D04314, doi:10.1029/2003JD003957, 2004.

26 Jacob, D.J. and Winner, D.A.: Effect of climate change on air quality, *Atmos. Environ.*, 43, 51-63,
27 2009.

28 Jacob, D., Petersen, J., Eggert, B., Alias, A., Christensen, O.B., Bouwer, L.M., Braun, A., Colette,
29 A., Déqué, M., Georgievski, G., Georgopoulou, E., Gobiet, A., Menut, L., Nikulin, G., Haensler,
30 A., Hempelmann, N., Jones, C., Keuler, K., Kovats, S., Kroner, N., Kotlarski, S., Kriegsmann, A.,
31 Martin, E., van Meijgaard, E., Moseley, C., Pfeifer, S., Preuschmann, S., Radermacher, C., Radtke,

1 K., Rechid, D., Rounsevell, M., Samuelsson, P., Somot, S., Soussana, J.-F., Teichmann, C.,
2 Valentini, R., Vautard, R., Weber, B. and Yiou, P.: EURO-CORDEX: new high-resolution climate
3 change projections for European impact research, *Reg. Environ. Change*, 14:563–578. DOI
4 10.1007/s10113-013-0499-2, 2014.

5 Jerrett, M., Finkelstein, M.M., Brook, J.R., Arain, M.A., Kanaroglou, P., Stieb, D.M., Gilbert,
6 N.L., Verma, D., Finkelstein, N., Chapman, K.R. and Sears, MR.: A cohort study of traffic-related
7 air pollution and mortality in Toronto, Ontario, Canada, *Environ. Health Perspect.*, 117 (5): 772-
8 777, 2009.

9 Johnson, C.E., Collins, W.J., Stevenson, D.S. and Derwent, R.G.: The relative roles of climate and
10 emissions changes on future oxidant concentrations, *J. Geophys. Res.* 104, 18,631–18,645, 1999.

11 Kahnert, M.: Variational data analysis of aerosol species in a regional CTM: background error
12 covariance constraint and aerosol optical observation operators, *Tellus* 60B: 753-770, 2008.

13 Katragkou E., Zanis, P., Kioutsioukis, I., Tegoulas, I., Melas, D., Krüger, B.C. and Coppola, E.:
14 Future climate change impacts on summer surface ozone from regional climate-air quality
15 simulations over Europe, *J. Geophys. Res.*, 116, D22307, doi:10.1029/2011JD015899, 2011.

16 Ketzel, M., Omstedt, G. and Johansson, C.: Estimation and validation of PM_{2.5}/PM₁₀ exhaust
17 and non-exhaust emission factors for practical street pollution modeling. *Atmos. Environ.*, 41 (40),
18 9370–9385, 2007.

19 Klimont, Z., Kupiainen, K., Heyes, C., Cofala, J., Rafaj, P., Höglund-Isaksson, L., Borken, J.,
20 Schöpp, W., Winiwarter, W., Purohit, P., Bertok, I. and Sander, R.: ECLIPSE V4a: global emission
21 data set developed with the GAINS model for the period 2005 to 2050. Key features and principal
22 data sources, available at: http://eccad.sedoo.fr/eccad_extract_interface/JSF/page_login.jsf (last
23 access: 30 September 2015), 2013.

24 Lacressonniere, G., Peuch, V.-H., Vautard, R., Arteta, J., Déqué, M., Joly, M., Josse, B., Marécal,
25 V. and Saint-Martin, D.: European air quality in the 2030s and 2050s: Impacts of global regional
26 emission trends and of climate change, *Atmos. Environ.*, 92, 348-358, 2014.

27 Lamarque, J.-F., Bond, T.C., Eyring, V., Granier, C., Heil, A., Klimont, Z., Lee, D., Liousse, C.,
28 Mieville, A., Owen, B., Schultz, M.G. Shindell, D., Smith, S.J., Stehfest, E., Van Aardenne, J.,
29 Cooper, O.R., Kainuma, M., Mahowald, N., McConnell, J.R., Naik, V., Riahi, K. and van Vuuren,
30 D.P.: Historical (1850–2000) gridded anthropogenic and biomass burning emissions of reactive
31 gases and aerosols: methodology and application, *Atmos. Chem. Phys.*, 10, 7017-7039, 2010.

1 Langner, J., Bergström, R. and Pleijel, K.: European scale modeling of sulfur, oxidised nitrogen
2 and photochemical oxidants. Model development and evaluation for the 1994 growing season.
3 Swedish Meteorological and Hydrological Institute, RMK No. 82, 71 pp. (with errata), 1998.

4 Langner, J., Bergström, R. and Foltescu, V.: Impact of climate change on surface ozone and
5 deposition of sulphur and nitrogen in Europe., *Atmos. Environ.*, 39, 1129-1141, 2005.

6 Langner, J., Engardt, M., Baklanov, A., Christensen, J. H., Gauss, M., Geels, C., Hedegaard, G.
7 B., Nuterman, R., Simpson, D., Soares, J., Sofiev, M., Wind, P. and Zakey, A.: A multi-model
8 study of impacts of climate change on surface ozone in Europe, *Atmos. Chem. Phys.*, 12, 10423-
9 10440, 2012a.

10 Langner, J., Engardt, M. and Andersson, C.: European summer surface ozone 1990-2100, *Atmos.*
11 *Chem. Phys.*, 12, 10097-10105, 2012b.

12 Lattuati, M.: Contribution a l'étude du bilan de l'ozone troposphérique a l'interface de l'Europe et
13 de l'Atlantique Nord: modelisation lagrangienne et mesures en altitude, Phd thesis, Université P.
14 M. Curie, Paris, France, 1997.

15 Lauwaet, D., Viaene, P., Brisson, E., van Lipzig, N.P.M., van Noije, T., Strunk, A., Van Looy, S.,
16 Veldeman, N., Blyth, L., De Ridder, K. and Janssen, S.: The effect of climate change and emission
17 scenarios on ozone concentrations over Belgium: a high-resolution model study for policy support,
18 *Atmos. Chem. Phys.*, 14, 5893–5904, 2014.

19 Lepeule, J., Laden, F., Dockery, D. and Schwartz J.: Chronic exposure to fine particles and
20 mortality: an extended follow-up of the Harvard Six Cities study from 1974 to 2009, *Environ.*
21 *Health Perspect.*, 120 (7): 965-970, 2012.

22 Liao, H., Chen, W.-T. and Seinfeld, J.H.: Role of climate change in global predictions of future
23 tropospheric ozone and aerosols, *J. Geophys. Res.*, 111, doi: 10.1029/2005JD006852, 2006.

24 Likhvar, V., Pascal, M., Markakis, K., Colette, A., Hauglustaine, D., Valari, M., Klimont, Z.,
25 Medina, S. and Kinney, P.: A multi-scale health impact assessment of air pollution over the 21st
26 century, *Sci. Total. Environ.*, 514, 439-449.

27 Markakis, K., Valari, M., Colette, A., Sanchez, O., Perrussel, O., Honore, C., Vautard, R., Klimont,
28 Z. and Rao, S.: Air quality in the mid-21st century for the city of Paris under two climate scenarios;
29 from the regional to local scale, *Atmos. Chem. Phys.* 14, 7323-7340, 2014.

1 Markakis, K., Valari, M., Perrussel, O., Sanchez, O. and Honore, H.: Climate forced air-quality
 2 modeling at urban scale: sensitivity to model resolution, emissions and meteorology, *Atmos.*
 3 *Chem. Phys.* 15, 7703-7723, 2015.

4 Megaritis, A.G., Fountoukis, C., Charalampidis, P.E., Denier van der Gon, H.A., Pilinis, C. and
 5 Pandis, S.N.: Linking climate and air quality over Europe: effects of meteorology on PM_{2.5}
 6 concentrations. *Atmos. Chem. Phys.*, 14, 10283-10298, 2014.

7 Menut, L., Schmechtig, C. and Marticorena, B.: Sensitivity of the sandblasting fluxes calculations
 8 to the soil size distribution accuracy, *J. Atmos. Ocean. Tech.*, 22 (12): 1875–1884, 2005.

9 Menut, L., Bessagnet, B., Khvorostyanov, D., Beekmann, M., Blond, N., Colette, A., Coll, I.,
 10 Curci, G., Foret, G., Hodzic, A., Mailler, S., Meleux, F., Monge, J.-L., Pison, I., Siour, G.,
 11 Turquety, S., Valari, M., Vautard, R. and Vivanco, M.G.: CHIMERE 2013: a model for regional
 12 atmospheric composition modelling, *Geosci. Model Dev.*, 6, 981–1028, doi:10.5194/gmd-6- 981-
 13 2013, 2013.

14 Nenes, A., Pilinis, C. and Pandis, S.: ISORROPIA: A new thermodynamic model for inorganic
 15 multicomponent atmospheric aerosols, *Aquatic Geochem.*, 4, 123–152, 1998.

16 Nolte, C.G., Gilliland, A.B., Hogrefe, C. and Mickley, L.J.: Linking global to regional models to
 17 assess future climate impacts on surface ozone levels in the United States, *J. Geophys. Res.*, 113,
 18 D14307, doi:10.1029/2007JD008497, 2008.

19 Omstedt, G., Bringfelt, B. and Johansson, C.: A model for vehicle-induced non-tailpipe emissions
 20 of particles along Swedish roads, *Atmos. Environ.*, 39 (33), 6088–6097, 2005.

21 Pascal, M., Corso, M., Chanel, O., Declecq, C., Badaloni, C., Cesaroni, G., Henschel, S., Maister,
 22 K., Haluza, D., Martin-Olmedo, P. and Medina S.: Assessing the public health impact of urban air
 23 pollution in 25 European cities: results of the Aphekom project, *Sci. Total Environ.*, 449, 390-400,
 24 2013.

25 Prather, M., Gauss, M., Berntsen, T., Isaksen, I., Sundet, J., Bey, I., Brasseur, G., Dentener, F.,
 26 Derwent, R., Stevenson, D., Grenfell, L., Hauglustaine, D., Horowitz, L., Jacob, D., Mickley, L.,
 27 Lawrence, M., von Kuhlmann, R., Muller, J.-F., Pitari, G., Rogers, H., Johnson, M., van Weele,
 28 M. and Wild, O.: Fresh air in the 21st century?, *Geophys. Res. Lett.*, 30, 1100,
 29 doi:10.1029/2002GL016285, 2003.

30 REVIHAAP: Review of evidence on health aspects of air pollution – REVIHAAP Project,
 31 available at: <http://www.euro.who.int/en/health-topics/environment-and-health/air-quality/>

publications/2013/review-of-evidence-on-health-aspects-of-air-pollution-revihaap-project-final-technical-report (last access: 30 September 2015), 2013.

Riahi, K., Rao, S., Krey, V., Cho, C., Chirkov, V., Fischer, G., Kindermann, G., Nakicenovic, N. and Rafaj, P.: RCP 8.5-A scenario of comparatively high greenhouse gas emissions, *Clim. Change*, 109, 33–57, 2011.

Robertson, L., Langner, J. and Engardt, M.: An Eulerian limited-area atmospheric transport model, *J. Appl. Meteor.* 38, 190-210, 1999.

Seinfeld, J.H. and Pandis, S.N.: *Atmospheric Chemistry and Physics: From Air Pollution to Climate Change*, 2nd ed. John Wiley and Sons, Hoboken, NJ, 2006.

Skamarock, W.C. and Klemp J.B.: A time-split non-hydrostatic atmospheric model, *J. Comput. Phys.*, 227, 3465–3485, 2008.

Sillman, S. and He, D.: Some theoretical results concerning O₃-NO_x-VOC chemistry and NO_x-VOC indicators, *J. Geophys. Res.*, 107, 4659, doi:10.1029/2001JD001123, 2002.

Sillman, S., Vautard, R., Menut, L. and Kley, D.: O₃-NO_x-VOC sensitivity and NO_x-VOC indicators in Paris: Results from models and Atmospheric Pollution over the Paris Area (ESQUIF) measurements, *J. Geophys. Res.*, 108, 8563, doi:10.1029/2002JD001561, 2003.

Simpson, D., Benedictow, A., Berge, H., Bergström, R., Emberson, L.D., Fagerli, H., Flechard, C.R., Hayman, G.D., Gauss, M., Jonson, J.E., Jenkin, M.E., Nyíri, A., Richter, C., Semeena, V. S., Tsyro, S., Tuovinen, J.-P., Valdebenito, A. and Wind, P.: The EMEP MSC-W chemical transport model – technical description, *Atmos. Chem. Phys.*, 12, 7825–7865, 2012.

Sjödin, A., Ekström, M. and Hammarström, U.: Implementation and Evaluation of the ARTEMIS Road Model for Sweden's International Reporting Obligations on Air Emissions, in *Proceedings of the 2nd Conference Environment & Transport including the 15th Conference of Transport & Air Pollution*, vol. 1, no. 107, pp. 375–382, Reims, France, June 2006.

Strandberg, G., Barring, L., Hansson, U., Jansson, C., Jones, C., Kjellström, E., Kolax, M., Kupiainen, M., Nikulin, G., Samuelsson, P., Ullerstig, A. and Wang, S.: CORDEX scenarios for Europe from the Rossby Centre regional climate model RCA4. SMHI reports, RMK 116. ISSN 0347-2116, 2014.

Szopa, S., Hauglustaine, D.A., Vautard, R. and Menut, L.: Future global tropospheric ozone changes and impact on European air quality, *Geophys. Res. Lett.*, 33, L14805, doi:10.1029/2006GL025860, 2006.

1 Szopa, S. and Hauglustaine, D.: Relative impacts of worldwide tropospheric ozone changes and
2 regional emission modifications on European surface-ozone levels, *CR Geosci.*, 339, 709-720,
3 2007.

4 Szopa, S., Balkanski, Y., Schulz, M., Bekki, S., Cugnet, D., Fortems-Cheiney, A., Turquety, S.,
5 Cozic, A., Deandreis, C., Hauglustaine, D., Idelkadi, A., Lathiere, J., Lefevre, F., Marchand, M.,
6 Vuolo, R., Yan, N. and Dufresne, J.-L.: Aerosol and ozone changes as forcing for climate
7 evolution between 1850 and 2100, *Clim. Dynam.*, 40, 2223-2250. 2013.

8 Valari, M. and Menut, L.: Does an Increase in Air Quality Models' Resolution Bring Surface
9 Ozone Concentrations Closer to Reality?, *J. Atmos. Ocean. Technol.*, 25, 1955-1968, 2008.

10 Vautard, R., Honoré, C., Beekmann, M. and Rouil, L.: Simulation of ozone during the August
11 2003 heat wave and emission control scenarios, *Atmos. Environ.*, 39 (16): 2957–2967, 2005.

12 Vautard R., Builtjes, P.H.J., Thunis, P., Cuvelier, C., Bedogni, M., Bessagnet, B., Honore, C.,
13 Moussiopoulos, N., Pirovano, G., Schaap, M., Stern, R., Tarasson, L. and Wind, P.: Evaluation
14 and intercomparison of Ozone and PM10 simulations by several chemistry transport models over
15 four European cities within the CityDelta project, *Atmos. Environ.*, 41 (1), 173-188, 2007.

16 Vautard, R., Gobiet, A., Sobolowski, S., Kjellström, E., Stegehuis, A., Watkiss, P., Mendlik, T.,
17 Landgren, O., Nikulin, G., Teichmann, C. and Jacob, D.: The European climate under a 2°C global
18 warming, *Environ. Res. Lett.*, 9, 034006, doi:10.1088/1748-9326/9/3/034006, 2014.

19 Watson, L., Lacressonnière, G., Gauss, M., Engardt, M., Andersson, C., Josse, B., Marécal, V.,
20 Nyiri, A., Sobolowski, S., Siour G. and Vautard, R.: The impact of meteorological forcings on gas
21 phase air pollutants over Europe, *Atmos. Environ.*, 119, 240–257, 2015.

22 Zanis, P., Katragkou, E., Tegoulas, I., Poupkou, A., Melas, D., Huszar, P. and Giorgi, F.:
23 Evaluation of near surface ozone in air quality simulations forced by a regional climate model over
24 Europe for the period 1991-2000, *Atmos. Environ.*, 45(36), 6489-6500, 2011.

1
2
3
4
5
6

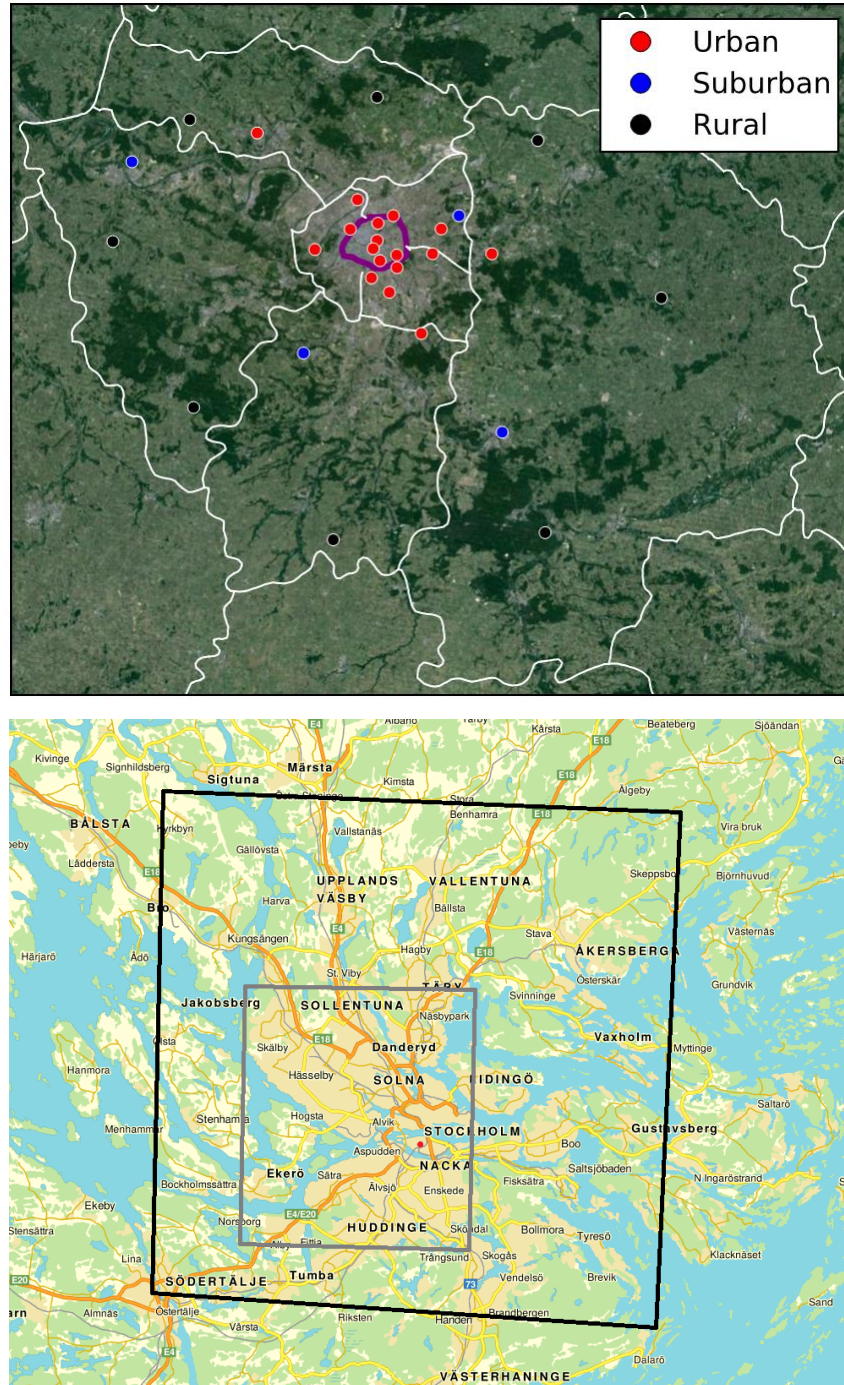


Figure 1. Top panel illustrates the IdF 4km resolution modeling domain, with the city of Paris in the centre (area enclosed by the purple line). Circles correspond to sites of the local air quality monitoring network (AIRPARIF) with red for urban, blue for suburban and black for rural. Bottom panel represents the Stockholm 1km resolution modeling domain (black outline) with the urban area enclosed in the grey rectangle. The red circle corresponds to the urban monitoring site.

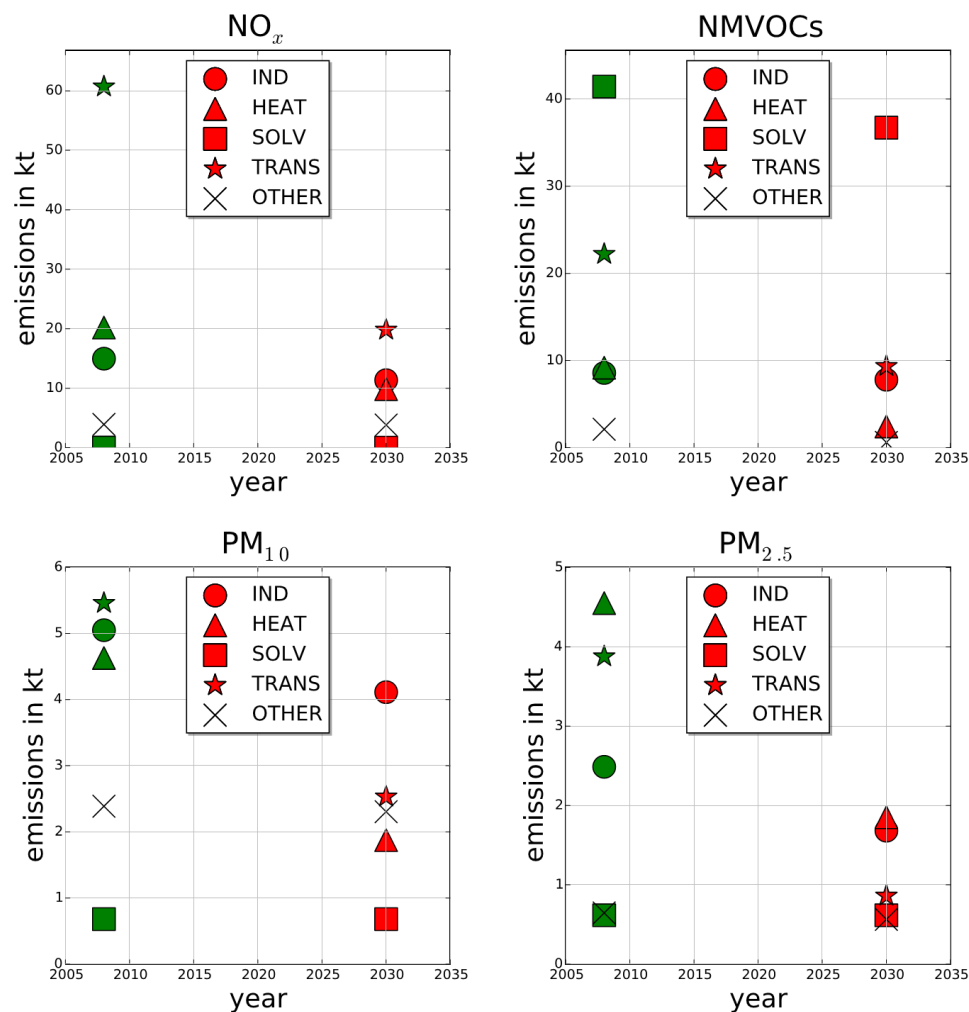
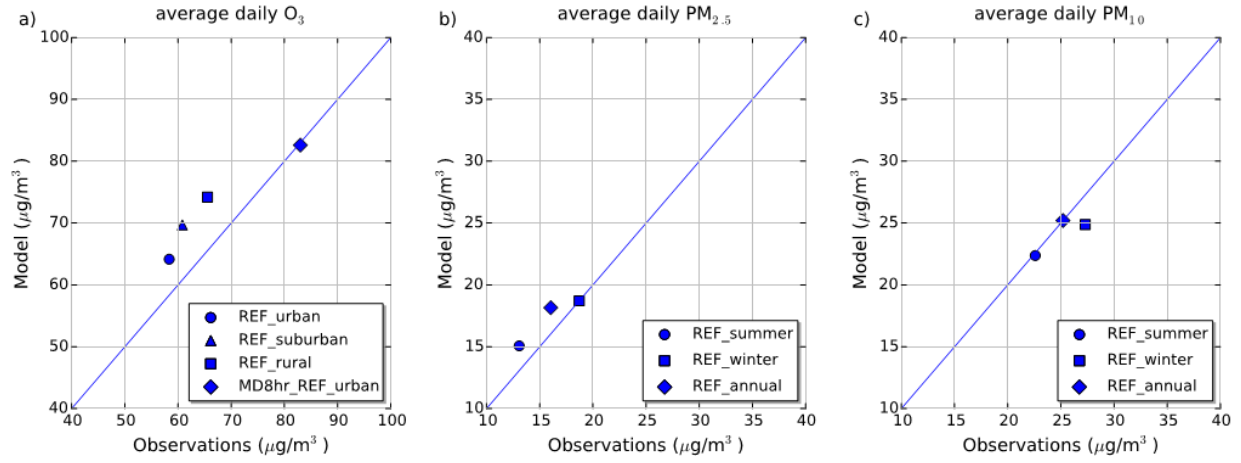


Figure 2. Annual present-time emissions of NO_x, NMVOCs, PM₁₀ and PM_{2.5} in IdF and their projections for 2030. IND corresponds to industrial emissions (SNAP1,3 and 4), HEAT to heating activities (SNAP2), SOLV to solvents use (SNAP6), TRANS to road and non-road transport (SNAP7 and 8) and OTHER represent the remaining source sectors (SNAP5,9 and 10).

1



2

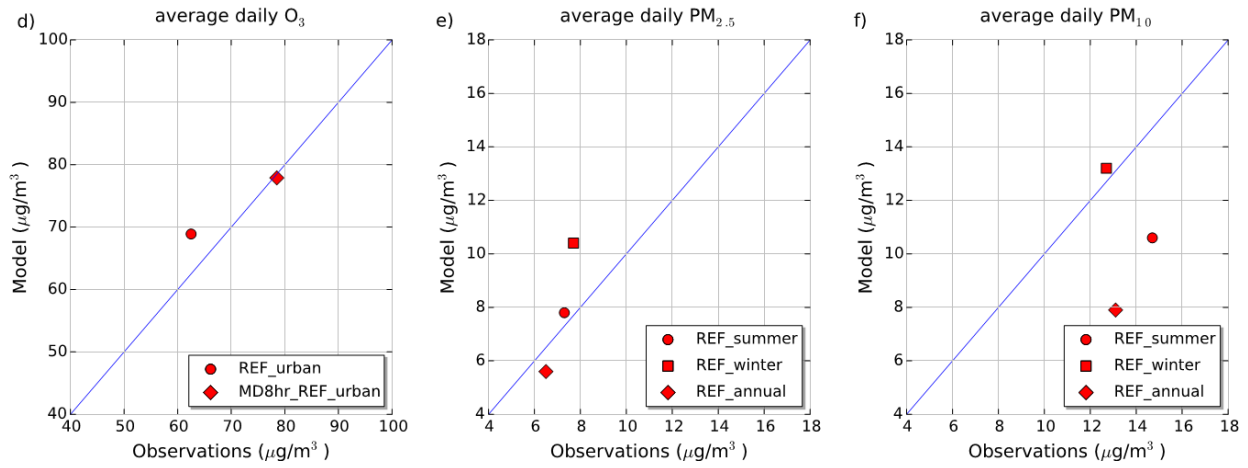
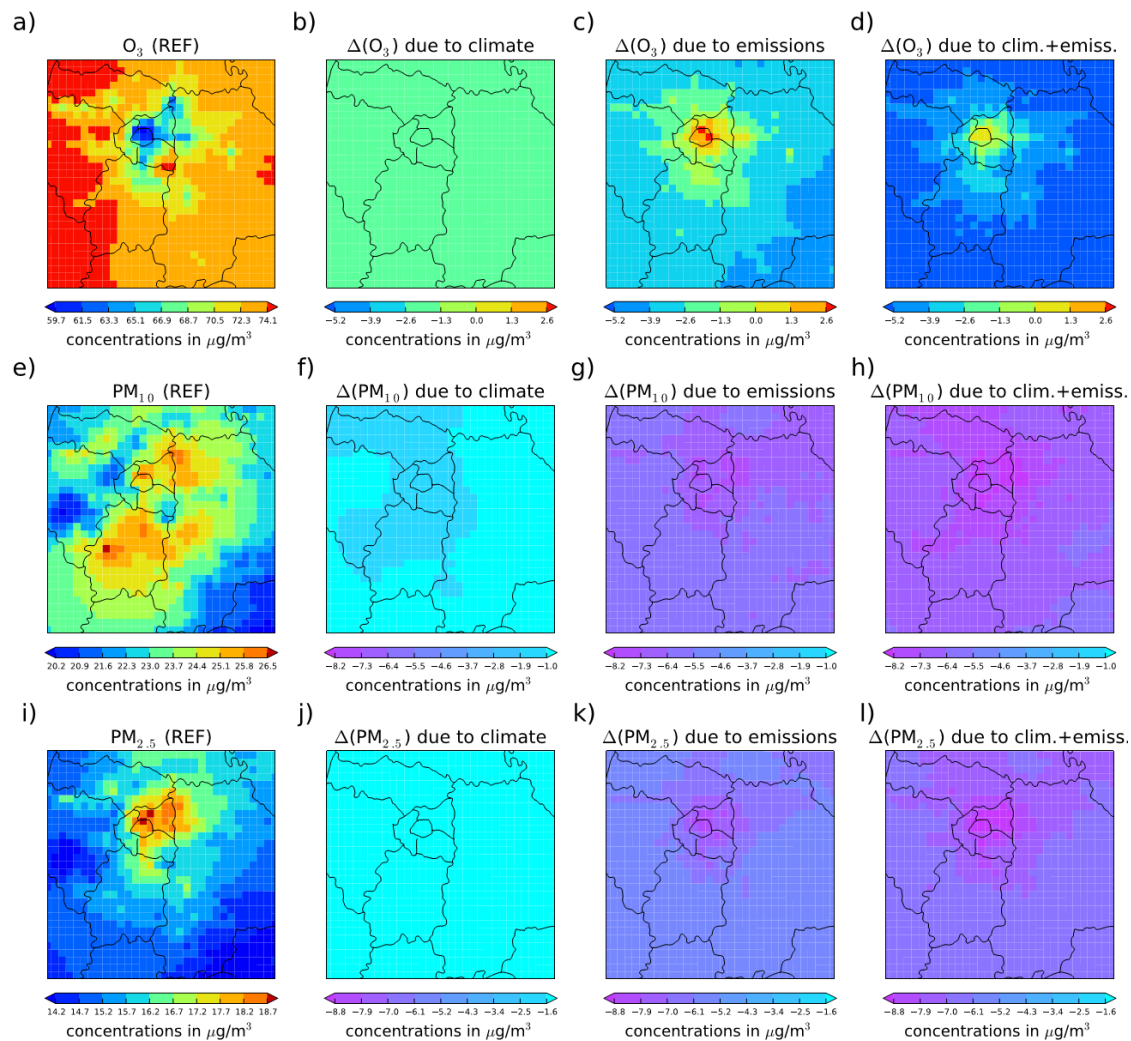


Figure 3. Ozone period (April-August) average ozone concentrations at urban, suburban and rural stations in IdF (panel a) and one urban station in the Stockholm area (panel d). The MD8hr values at urban locations are also shown (MD8hr_REF_urban). Average $PM_{2.5}$ and PM_{10} concentrations in wintertime (DJF), summertime (JJA) and on annual basis over urban stations in IdF are shown in panels b,c (panels e,f for Stockholm).

1



2

Figure 4. April-August mean ozone, annual mean PM_{10} and annual mean $PM_{2.5}$ concentration maps ($\mu g/m^3$) for IdF, expressed as absolute values at present-time (a,e,i) and as deltas between present-time and 2050 due to climate change (b,f,j), emissions changes (c,g,k) and the cumulative effect (d,h,l).

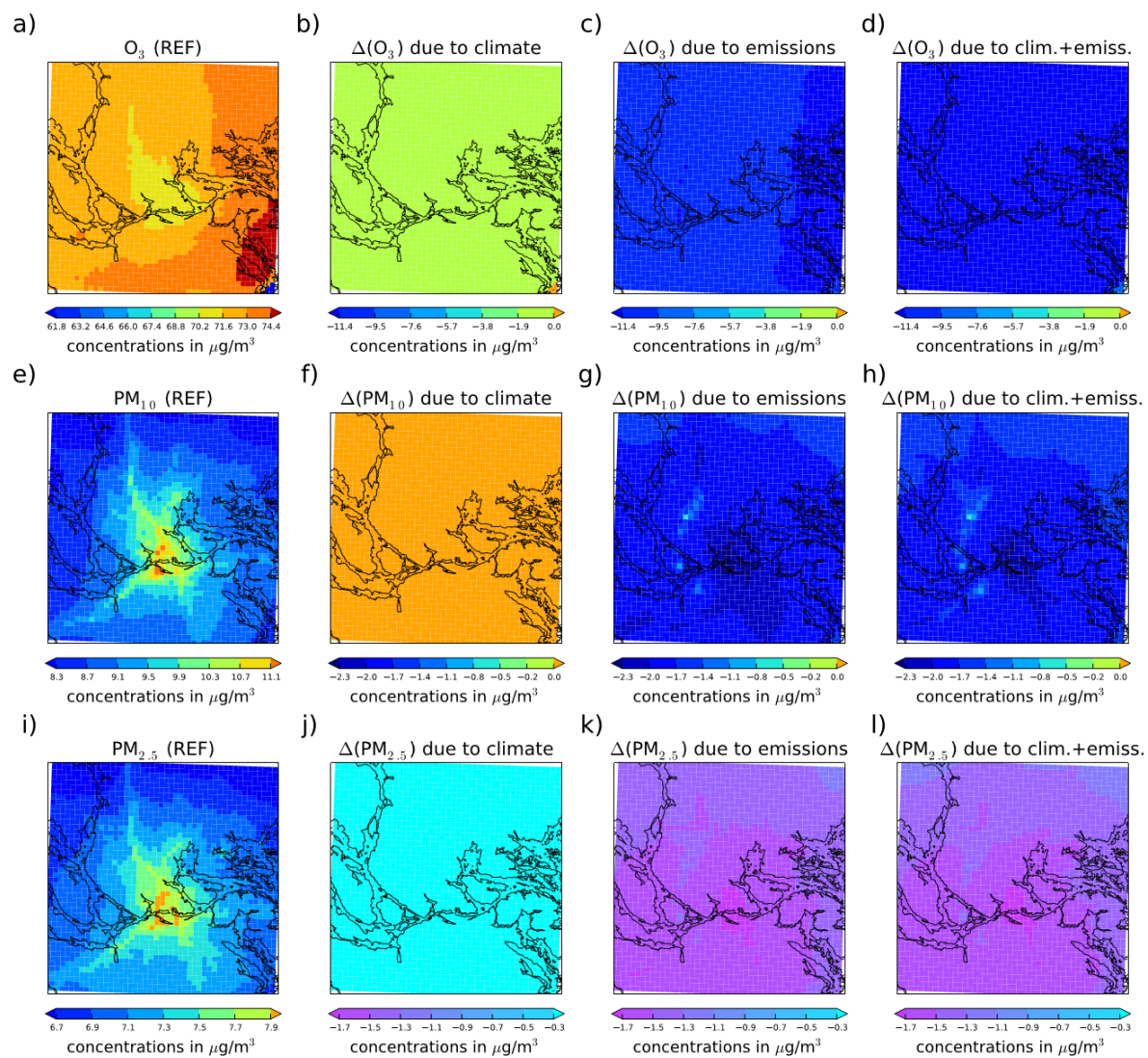


Figure 5. Similar to Fig. 4 for Stockholm.

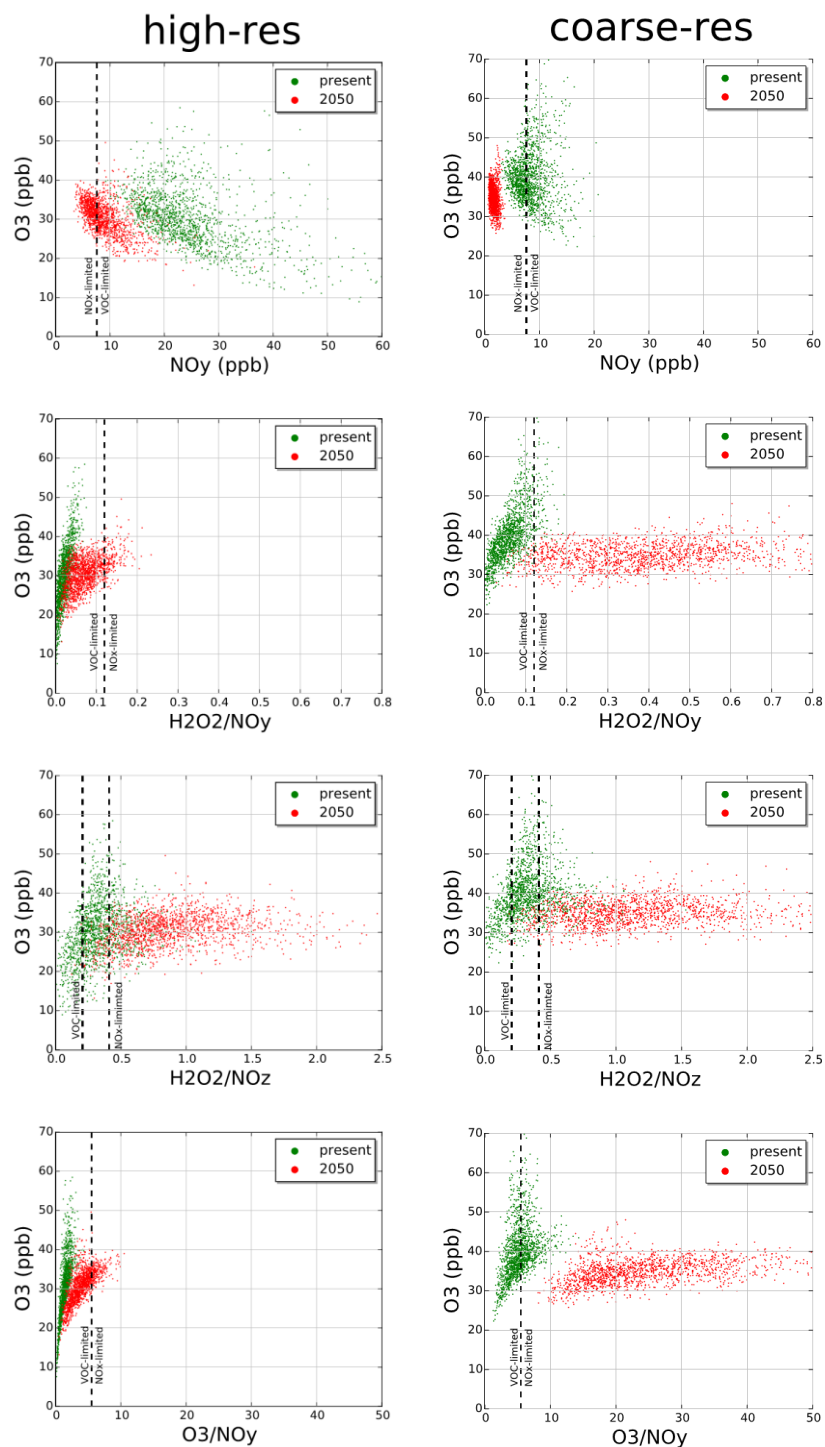


Figure 6. Scatter plots of daily average ozone concentrations (y-axis) against chemical regime indicators (x-axis) for the present and future runs in Paris. Results are presented for the high-resolution (left panels) and the coarse-resolution (right panels) applications. Dots correspond to daily average concentrations for each day of the ozone period. For each indicator the limit value that separates the regimes is also depicted with a dashed line.